Inorg. Chem. **2007**, *46*, 11183–11189

Asymmetrical Polar Modification of a Bivanadium-Capped Keggin POM by Multiple Cu–N Coordination Polymeric Chains

Jing-quan Sha,[†,‡] Jun Peng,*[,†] Hong-sheng Liu,[†] Jing Chen,[†] Ai-xiang Tian,[†] and Peng-peng Zhang[†]

Key Laboratory of Polyoxometalate Science of Ministry of Education, Faculty of Chemistry, Northeast Normal University, Changchun, Jilin 130024, P. R. China, and Faculty of Chemistry and Pharmacy, Jiamusi University, Jiamusi, HeilongJiang 154007, P. R. China

Received July 19, 2007

An unprecedented asymmetrically modified bivanadium-capped Keggin polyoxometalate (POM), $\{AsMo_{12}O_{40}(VO)[VO(H_2O)]\}\cdot[Cu(4,4'\text{-bipy})]_5\cdot H_2O$ (**1**) (bipy = bipyridine), has been hydrothermally synthesized and structurally characterized by a routine technique. Single-crystal X-ray diffraction analysis reveals that compound **1** exhibits a unique (3,4,6)-connected 3D framework with a $(6^2\cdot8^1)_2(8^3)_2(6^4\cdot8^2)_2(6^1\cdot8^{14})$ topology, constructed from $\{AsMo_{12}O_{40}(VO)[VO(H_2O)]\}^{5-}$ polyoxoanions modified by six $\{Cu(bipy)\}_n$ coordination polymeric chains. The asymmetrical polar coordination mode has never been found in the POM chemistry hitherto. It is also the first example of the bivanadium-capped POM as an anionic template to construct a 3D framework with the highest connection number of bicapped POMs. Additionally, by just changing the length of the organic ligand, a new compound $\{[AsMo_{12}O_{40}(VO)_2][Cu(bpe)]_2\}\cdot[Cu(bpe)]\cdot[H_2bpe]\cdot H_2O$ (**2**) (bpe = bis(4-pyridyl)ethylene), has been obtained, in which the $\{AsMo_{12}O_{40}(VO)_2\}$ sections are modified by double monotrack $\{Cu(bpe)\}_n$ coordination polymeric chains to form a "rail-like" 1D structure.

Introduction

The modification of the surfaces of polyoxometalate (POM) clusters has attracted much attention because many of their intriguing structural chemistry qualities and potential applications in such areas as molecular devices, biochemistry, and catalysts are directly related to their surface characteristics.[1] A promising approach toward the synthesis of this kind of hybrid lies in the proper selection of POMs as building blocks and transition-metal (TM) complexes as structure-directing and functional components. POMs have capability of coordinating to TM complexes to form extended POM frameworks because of the large number of their surface oxygen atoms. Recently, many hybrids made of POMs associated with various TM complexes have been reported by Zubieta,[2] Pope,[3] Wang,[4] Long,[5] and Niu,[6] and others. These researchers, as well as our own,[7] have indicated that POMs, organic ligands, and TM ions all play important

* To whom correspondence should be addressed. E-mail: jpeng@nenu.edu.cn or pjun56@yahoo.com.
† Northeast Normal University.
‡ Jiamusi University.

(1) (a) Gouzerh, P.; Proust, A. *Chem. Rev.* **1998**, *98*, 77−112. (b) Hill, C. L. *Chem. Rev.* **1998**, *98*, 1−2. (c) Long, D. L.; Abbas, H; Kögerler, P.; Cronin, L. *Angew. Chem., Int. Ed.* **2005**, *44*, 3415−3419. (d) Velessiotis, D.; Glezos, N.; Ioannou-Sougleridis, V. *J. Appl. Phys.* **2005**, 98. (e) Bielanski, A.; Lubanska, A.; Micek-Ilnicka, A.; Pozniczek, J. *Coord. Chem. Rev.* **2005**, *249*, 2222−2231. (f) Wu, P. E.; Li, Q.; Wei, Y. G.; Wang, Y.; Wang, P.; Guo, H. Y. *Eur. J. Inorg. Chem.* **2004**, 2819−2822. (g) Wei, Y. G.; Xu, B. B; Barnes, C. L.; Peng, Z. H. *J . Am. Chem. Soc.* **2001**, *123*, 4083−4084. (h) Li, Q.; Wei, Y. G.; Hao, J.; Zhu, Y. L.; Wang, L. S. *J. Am. Chem. Soc.* **2007**, *129*, 5810−5811.

(2) (a) Hagrman, P. J.; Hagrman, D.; Zubieta, J. *Angew. Chem., Int. Ed.* **1999**, *38*, 2638−2684. (b) Burkholder, E.; Golub, V.; O'Connor, C. J.; Zubieta, J. *Inorg. Chem.* **2003**, *42*, 6729−6740. (c) Burkholder, E.; Golub, V.; O'Connor, C. J.; Zubieta, J. *Chem. Commun.* **2003**, 2128−2129. (d) Burkholder, E.; Golub, V.; O'Connor, C. J.; Zubieta, J. *Inorg. Chem. Commun.* **2004**, *7*, 363−366.

(3) (a) Masahiro, S.; Dickman, M. H.; Pope, M. T. *Angew. Chem., Int. Ed.* **2000**, *39*, 2914−2916. (b) Wei, X. Y.; Dickman, M. H.; Pope, M. T. *J. Am. Chem. Soc.* **1998**, *120*, 10254−10255.

(4) (a) Wang, X. L.; Qin, C.; Wang, E. B.; Su, Z. M.; Li, Y. G.; Xu, L. *Angew. Chem., Int. Ed.* **2006**, *45*, 7411−7414. (b) An, H. Y.; Xiao, D. R.; Wang, E. B.; Li, Y. G.; Su, Z. M.; Xu, L. *Angew. Chem., Int. Ed.* **2006**, *45*, 904−908.

(5) (a) Ren, Y. P.; Kong, X. J.; Hu, X. Y.; Sun, M.; Long, L. S. *Inorg. Chem.* **2006**, *45*, 4016−4024. (b) Ren, Y. P.; Kong, X. J.; Long, L. S.; Huang, R. B.; Zheng, L. S. *Cryst. Growth Des.* **2006**, *6*, 572−576. (c) Kong, X. J; Ren, Y. P.; Zheng, P. Q.; Long, Y. X.; Long, L. S., Huang, R. B.; Zheng, L. S. *Inorg. Chem.* **2006**, *45*, 10702−10711.

(6) (a) Niu, J. Y.; Wang, Z. L.; Wang, J. P. *Inorg. Chem. Commun.* **2003**, *6*, 1272−1274. (b) Devi, R. N.; Burkholder, E.; Zubieta, J. *Inorg. Chem. Acta* **2003**, *348*, 150−156. (c) Niu, J. Y.; Wang, Z. L.; Wang, J. P. *Polyhedron* **2004**, *23*, 773−777. (d) Wang, J. P.; Ma, P. T.; Niu, J. Y. *Inorg. Chem. Commun.* **2006**, *9*, 1049−1052.

(7) Dong, B. X.; Peng, J.; Gomez-Garcia, C. J.; Benmansour, S.; Jia, H.Q.; Hu, N.H. *Inorg. Chem.* **2007**, *46*, 5933−5941.

10.1021/ic7014308 CCC: $37.00
Published on Web 11/16/2007

roles in the self-assembly processes. The controllable extension and the functionalization of POM frameworks still remain a challenge. Generally, to stabilize the structures of modified POMs, the symmetrical coordination of the POMs is favorable. Only a few examples involving the asymmetrically modified structure were reported up to now,[8] and the asymmetrical surface modification of POMs remains an attractive research topic.

According to the basic concept, as the charge density on the surface oxygen atoms of POMs increases, a significant affinity for the polyoxoanions to coordinate to TM complexes should appear. As a result, the POMs may be modified by more TM complexes via the surface oxygen atoms of the POMs. A frequent and effective method for obtaining such highly negative charged polyoxoanions is to reduce the component metals from the highest oxidation state to a lower one, i.e., $Mo(W)^{VI} \rightarrow Mo(W)^{V}$, or alternatively, to replace the metals of a high oxidation state with those of a low oxidation state, i.e., $Mo(W)^{VI} \rightarrow Cu^{II}$.[9]

During our efforts to modify asymmetrically and to functionalize POM frameworks, the bivanadyl-capped Keggin POMs[10] have captured our attention for the following reasons: (a) Capping of the {VO} units on two opposite $\{M_4O_4\}$ windows of the Keggin POMs results in an asymmetrical negative charge distribution and polarization of the POM globe. This offers an opportunity to modify the POM in an asymmetrical coordination mode. (b) The steric orientations of the coordination sites for the capped Keggin POMs are more flexible than those for the uncapped ones because of the vanadyl groups. (c) The partly metal centers of the bicapped Keggin POMs often possess a lower oxidation state. The addition of electrons to the cluster strongly modifies the absolute energy of the molecular orbitals[11] and activates the surface oxygen atoms, making a covalent graft of the POM with ease. More recently, the bivanadyl-capped Keggin $[PMo_{12}O_{40}(VO)_2]^{q-}$ was proposed as a model of spin qubits with electrically gated polyoxometalate molecules.[12] The potential application perspective further stimulated our interest in the species of the bivanadyl-capped Keggin POMs.

In fact, we have empirically synthesized a dozen TM cation modified bivanadyl-capped Keggin POMs[13] and other POMs[7] and found that the coordination nature of the TM ions also plays a key role in the assembly process. Cu ions usually behave with changeable oxidation states and versatile coordination geometries under hydrothermal conditions; in particular, Cu^+ ions can adopt "see-saw", T-type, and linear coordination geometries, and so on. So Cu^+ is a good candidate for the asymmetrical surface modification of POMs. On the basis of the aforementioned points and the continual research of new high-dimensional hybrid compounds based on high-connectivity POMs, we have tried to choose bivanadium-capped Keggin POMs as templates/ligands and Cu−N coordination complexes as building units/modifiers to constitute the assemblies of TM cation−POM coordination polymers with complicated structures. We report here the bicapped Keggin $\{AsMo_{12}O_{40}(VO)[VO(H_2O)]\}^{5-}$ cluster multiply modified by six $\{Cu(bipy)\}_n$ chains, formulated as $\{AsMo_{12}O_{40}(VO)[VO(H_2O)]\}\cdot[Cu(4,4'\text{-bipy})]_5\cdot H_2O$ (**1**) (bipy = bipyridine), which exhibits an unusually asymmetrical polar surface modification and a unique (3,4,6)-connected 3D framework. Additionally, by just changing the length of the organic ligand, a "rail-like" 1D assembly, formulated as $\{[AsMo_{12}O_{40}(VO)_2][Cu(bpe)]_2\}\cdot[Cu(bpe)]\cdot[H_2\text{-bpe}]\cdot H_2O$ (**2**) (bpe = bis(4-pyridyl)ethylene), has been obtained, which gives another example to observe the effect of the organic ligand length.

Experimental Section

Materials and Methods. All reagents were purchased commercially and used without further purification. Elemental analyses (C, H, and N) were performed on a Perkin-Elmer 2400 CHN elemental analyzer and on a Leaman inductively coupled plasma spectrometer (Cu, Mo, and V). The IR spectra were obtained on an Alpha Centaurt FT/IR spectrometer with KBr pallet in the 400−4000 cm^{-1} region. X-ray photoelectron spectroscopy (XPS) analyses were performed on a VGESCALABMK II spectrometer with a Mg Kα (1253.6 eV) achromatic X-ray source. The vacuum inside the analysis chamber was maintained at 6.2×10^{-6} Pa during analysis. Cyclic voltammograms were obtained with a CHI 660 electrochemical workstation at room temperature. Platinum gauze was used as a counter electrode, and the Ag/AgCl electrode was the reference electrode. Chemically bulk-modified carbon-paste electrodes (CPEs) were used as the working electrodes.

The compounds **1** and **2** modified CPEs (**1**−CPE and **2**−CPE) were fabricated as follows: 48 mg of graphite powder and 8 mg of **1** or **2** were mixed and ground together by an agate mortar and pestle to achieve a uniform mixture, and then was added 0.6 mL of Nujol with stirring. The homogenized mixture was packed into a glass tube with a 1.2 mm inner diameter, and the tube surface was wiped with paper. Electrical contact was established with a copper rod through the back of the electrode.

Syntheses. $\{AsMo_{12}O_{40}(VO)[VO(H_2O)]\}\cdot[Cu(4,4'\text{-bipy})]_5\cdot H_2O$ **(1).** A mixture of $Li_3[AsMo_{12}O_{40}]\cdot xH_2O$ (303 mg),[14] $Cu(NO_3)_2\cdot 3H_2O$ (67.3 mg), 4,4′-bpy (57 mg), NH_4VO_3 (35 mg), triethylamine (trea) (60 mg), and H_2O (10 mL) in a molar ratio of 1:2:2:2:4:4000 was stirred for 1 h in air. The pH was then adjusted to 4.3 with 1 M HCl, and the mixture was transferred to an 18 mL Teflon-lined reactor. After 6 days of heating at 165 °C, the reactor was slowly cooled to room temperature over a period of 16 h. Blocklike black-brown crystals of **1** were filtered, washed with water, and dried at room temperature. Yield: 0.068 g (39% based on Cu). Anal. Calcd for $C_{50}H_{44}AsCu_5Mo_{12}N_{10}O_{44}V_2$ (3134.70): C 19.14,

(8) (a) Ritchie, C.; Burkholder, E.; Kögerler, P.; Cronin, L. *Dalton Trans.* **2006**, 1712−1714. (b) Sha, J. Q.; Peng, J.; Liu, H. S.; Chen, J.; Dong, B. X.; Tian, A. X.; Su, Z. M. *Eur. J. Inorg. Chem.* **2007**, 1268−1274.
(9) Felices, L. S.; Vitoria, P.; Gutiérrez-Zorrilla, J. M.; Lezama, L.; Reinoso, S. *Inorg. Chem.* **2006**, *45*, 7748−7757.
(10) Chen, Q.; Hill, C. L. *Inorg. Chem.* **1996**, *35*, 2403−2405.
(11) Maestre, J. M.; Poblet, J. M.; Bo, C.; Casañ-Pastor, N.; Gomez-Romero, P. *Inorg. Chem.* **1998**, *37*, 3444−3446.
(12) Lehmann, J.; Galta-arino, A.; Coronado, E.; Loss, D. *Nat. Nanotechnol.* **2007**, *2*, 312−317.
(13) (a) Shi, Z. Y.; Gu, X .J.; Peng, J.; Yu, X.; Wang, E. B. *Eur. J. Inorg. Chem.* **2006**, 385−388. (b) Shi, Z. Y.; Gu, X. J.; Peng, J.; Chen, Y. H. *J. Solid State Chem.* **2005**, *178*, 1988−1995. (c) Shi, Z. Y.; Peng, J.; Gomez-Garcia, C. J.; Benmansour, S.; Gu, X. J. *J. Solid State Chem.* **2006**, *179*, 253−265. (d) Gu, X. J.; Peng, J.; Shi, Z. Y.; Chen, Y. H.; Han, Z. G.; Wang, E. B.; Ma, J. F. *Inorg. Chim. Acta* **2005**, *358*, 3701−3710.
(14) Sanchez, C.; Livage, J.; Launary, J. P.; Fournier, M.; Jeannin, Y. *J. Am. Chem. Soc.* **1982**, *104*, 3194−3202.

Table 1. Crystal Data and Structure Refinements for **1** and **2**

	compound	
	1	**2**
formula	$C_{50}H_{44}AsCu_5Mo_{12}N_{10}O_{44}V_2$	$C_{48}H_{44}AsCu_3Mo_{12}N_8O_{43}V_2$
M_r	3134.70	2939.61
cryst syst	monoclinic	triclinic
space group	$P2_1/n$	$P\bar{1}$
a/Å	13.8849(6)	12.274(4)
b/Å	21.6767(9)	12.872(4)
c/Å	25.4158(11)	13.108(4)
α/deg	90	93.971(5)
β/deg	99.2810(10)	104.876(4)
γ/deg	90	110.758(5)
V/Å^3	7549.5(6)	1842.0(10)
T/K	293(2)	293(2)
Z	4	1
D_c/Mg/m^{-3}	2.726	2.645
μ(Mo Kα)/mm^{-1}	4.063	3.599
total reflns	34 879	8920
indep reflns	13 886	6200
R_{int}	0.0436	0.0362
R_1 [$I > 2\sigma(I)$][a]	0.0534	0.0782
R_2 [$I > 2\sigma(I)$][b]	0.1464	0.1734

[a] $R_1 = \sum||F_o| - |F_c||/\sum|F_o|$. [b] $R_2 = \{\sum[w(F_o^2 - F_c^2)^2]/\sum[w(F_o^2)^2]\}^{1/2}$.

H 1.4, N 4.47, Cu 10.21, Mo 36.81, V 3.26. Found: C 19.09, H 1.34, N 4.42, Cu 10.14, Mo 36.59, V 3.15.

{[AsMo$_{12}$O$_{40}$(VO)$_2$][Cu(bpe)]$_2$}·[Cu(bpe)]·[H$_2$bpe]·H$_2$O (2). Compound **2** was prepared in a manner similar to that described for **1**, except the bpe ligand replaced the bipy ligand. The yield is 0.054 g (21% based on Cu). Anal Calcd for $C_{48}H_{44}AsCu_3Mo_{12}N_8O_{43}V_2$ (2939.61): C 19.61, H 1.50, N 3.81, Cu 6.54, Mo 39.22, V 3.47. Found: C 19.59, H 1.53, N 3.78, Cu 6.48, Mo 39.16, V 3.39.

X-ray Crystallographic Study. The crystal data for compounds **1** and **2** were collected on a Bruker SMART-CCD diffractometer and a Rigaku RAXIS RAPID IP diffractometer, respectively, with Mo Kα monochromatic radiation (λ = 0.71073 Å) at 293 K. All structures were solved by direct methods and refined by full matrix least squares on F^2 using the *SHELXTL* crystallographic software package.[15] All the non-hydrogen atoms were refined anisotropically. The positions of hydrogen atoms on carbon atoms were calculated theoretically. The crystal data and structure refinements of compounds **1** and **2** are summarized in Table 1. Selected bond lengths and angles for compounds **1** and **2** are listed in Tables S1 and S2 (Supporting Information). The CCDC reference numbers are 626196 for **1** and 633795 for **2**.

Results and Discussion

Structure Description of Compound 1. Single-crystal X-ray diffraction analysis reveals that **1** shows a complicated 3D structure, which is constructed by one {AsMo$_{12}$O$_{40}$(VO)[VO(H$_2$O)]} cluster (abbreviated to {AsMo$_{12}$V$_2$}), five Cu(bipy) coordination complexes, and one water molecule. The {AsMo$_{12}$V$_2$} cluster, similar to those of [XMo$_{12}$O$_{40}$(VO)$_2$] (X = P, Si, Ge),[13] can be best described as the α-Keggin core {AsMo$_{12}$O$_{40}$} capped by {VO} and {VO(H$_2$O)} groups on two opposite {Mo$_4$O$_4$} pits of the {AsMo$_{12}$O$_{40}$} (Figure 1). The tau trigonality factor (τ), used to quantify the

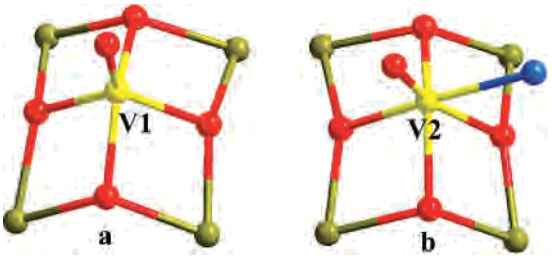

Figure 1. Ball-and-stick representation of the coordination environments of the V atoms in **1**. The color code is as follows: Mo, brown; V, yellow; O, red; and O (H$_2$O), blue.

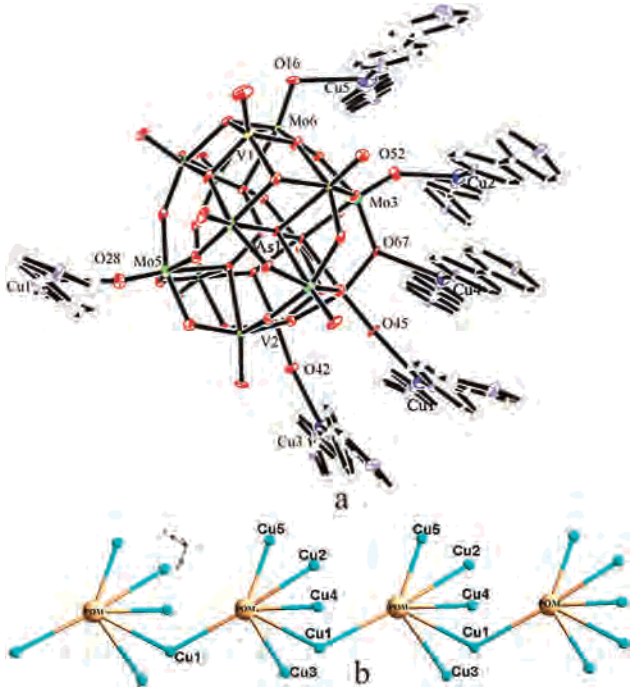

Figure 2. (top) ORTEP drawing of the {AsMo$_{12}$V$_2$} cluster modified in an unusually asymmetrical coordination mode at the 30% probability level in **1**. Only some atoms are labeled, and water molecules and all hydrogen atoms are omitted for clarity. (bottom) Schematic view of the 1D structure constructed by {AsMo$_{12}$V$_2$} clusters and five Cu atoms. The color code is as follows: {AsMo$_{12}$V$_2$}, buff; and Cu, blue.

geometrical distortion for the five-coordination V atoms, is 0.46 in **1**, which falls between 1 and 0, indicating that the coordination geometry of the V atoms is intermediate between that of square pyramidal and trigonal bipyramidal.[16] The bond lengths of V−O range from 1.591(7) to 2.006 (6) Å, and the O−V−O angles are in the range of 75.1(3)−123.9(4)°. The V2 atom adopts a distorted octahedral coordination geometry with the bond lengths of V−O from 1.624(7) to 2.067(6) Å, the bond length of V−OH$_2$ equals 2.221(6) Å, and the O−V−O angles are in the range of 74.9(2)−138.3(3)°. Such different coordination modes in bivanadium-capped Keggin POMs have never been reported.

The five crystallographically unique Cu atoms are coordinated by 4,4′-bipy to form four parallel {Cu(bipy)}$_n$ chains, among which Cu3, Cu4, and Cu5 each form a chain, while Cu1 and Cu2 are alternately arrayed to form one chain (shown in Figure S1, Supporting Information).

(15) (a) Sheldrick, G. M. *SHELX-97, Program for Crystal Structure Refinement*; University of Göttingen: Göttingen, Germany, 1997. (b) Sheldrick, G.M. *SHELXL-97, Program for Crystal Structure Solution*; University of Göttingen: Göttingen, Germany, 1997.

(16) Addison, A. W.; Rao, T. N. *J. Chem. Soc., Dalton Trans.* **1984**, 1349−1356.

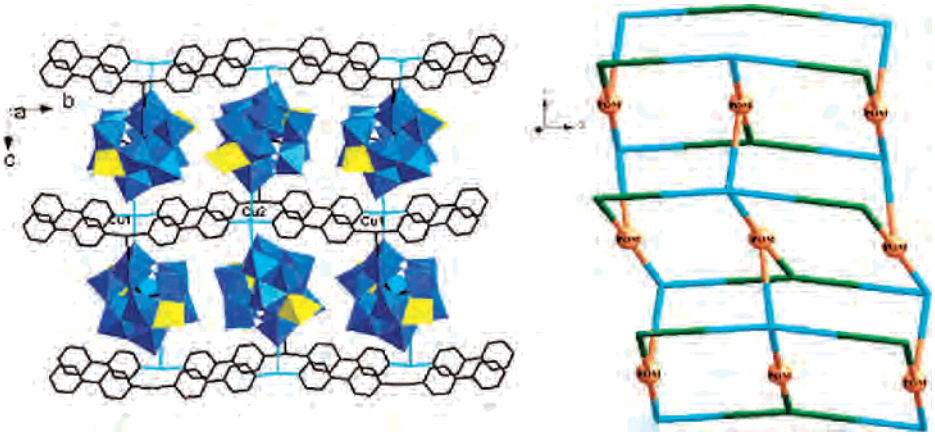

Figure 3. (left) View of the 2D structure constructed by $\{AsMo_{12}V_2\}$ clusters and Cu1···Cu2···Cu1 chains in **1**. (right) Schematic view of the $(6^2{\cdot}8^1)$-$(6^2{\cdot}8^1)(6^4{\cdot}8^2)$ topology. The color code is as follows: Cu1, blue; Cu2, green; and $\{AsMo_{12}V_2\}$, brown.

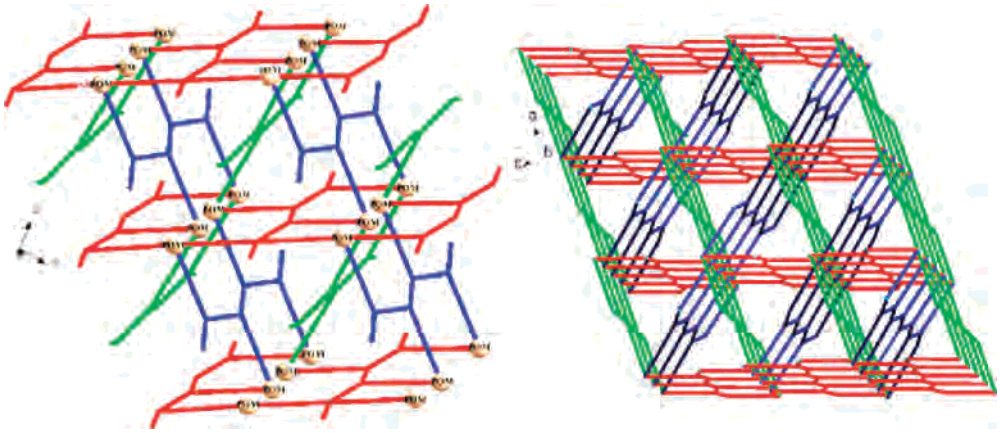

Figure 4. (left) Schematic view of the 3D framework constructed from $\{Cu(bipy)\}_n$ chain-modified POMs for Cu3, Cu4, and Cu5 in **1**. (right) Schematic view of the $(8^3)_4$ topology.

One fascinating structural feature for compound **1** is that the $\{AsMo_{12}V_2\}$ globe is modified in an unusually asymmetrical mode as shown in Figure 2 (top). The $\{AsMo_{12}V_2\}$ cluster acts as a hexadentate inorganic ligand, providing one O atom from the $\{VO(H_2O)\}$ group and the other five atoms from the terminal and bridge O atoms of the $\{AsMo_{12}V_2\}$ cluster and coordinating to six Cu^+ centers. Among the six Cu^+ centers, Cu1 adopts a tetracoordinated see-saw geometry, achieved by two N atoms of two 4,4′-bipy ligands and two O atoms of two $\{AsMo_{12}V_2\}$ clusters; Cu2, Cu3, Cu4, and Cu5 adopt a three-coordinated T-shaped geometry, accomplished by two N atoms of two 4,4′-bipy ligands and one O atom of a $\{AsMo_{12}V_2\}$ cluster. The bond distances of Cu−O are between 2.252(7) and 2.520 Å, and the bond angles of N−Cu−N and N−Cu−O are 160.4(4)−170.4(3)° and 93.5(3)−98.3(3)°, respectively. The modified POM clusters are linked together by the sharing of the Cu1 atom, resulting in a POM···Cu1···POM chain (Figure 2, bottom). This uncommon coordination pattern has never been observed.

Another interesting structural feature is the 2D framework, which is constructed from approximately perpendicular cross chains of $(POM{\cdots}Cu1{\cdots}POM)_n$ and $\{Cu(bipy)\}_n$, as shown in Figure 3 (left). In the layer, each $\{AsMo_{12}V_2\}$cluster bonds to the Cu1 and Cu2 atoms through three corner-sharing Cu−O−Mo bridges (O28 and O52 for Cu1, O45 for Cu2); thus, three $\{Cu(bipy)\}_n$ coordination polymer chains are linked together by $\{AsMo_{12}V_2\}$clusters to achieve a 2D structure. Consequently, the $\{AsMo_{12}V_2\}$cluster and Cu2 atom serve as three-connected nodes, and Cu1 serves as a four-connected node, resulting in a $(6^2{\cdot}8^1)(6^2{\cdot}8^1)(6^4{\cdot}8^2)$ topology (Figure 3, right).

Furthermore, the remaining $\{Cu(bipy)\}_n$ chains bind to the $\{AsMo_{12}V_2\}$clusters via corner-sharing Cu−O−Mo bridges for Cu4 and Cu5 and the Cu−O−V bridge for Cu3. In this way, the $\{AsMo_{12}V_2\}$ clusters become pendants of the $\{Cu(bipy)\}_n$ chains, projecting toward two sides of the chains (Figure S2, Supporting Information). The chains with the POM pendants are packed in a staggered fashion, resulting in a complicated 3D structure (Figure 4, left). In the 3D framework, $\{AsMo_{12}V_2\}$clusters and Cu3, Cu4, and Cu5 atoms serve as three-connected nodes to form a $(8^3)_4$ topology (Figure 4, right).

In summary, the $\{AsMo_{12}V_2\}$ clusters exhibit an asymmetrical polar modification by six $\{Cu(bipy)\}_n$ coordination polymers, generating an unique (3,4,6)-connected 3D framework with an unprecedented $(6^2{\cdot}8^1)_2(8^3)_2(6^4{\cdot}8^2)_2(6^1{\cdot}8^{14})$ topology (Figure 5). In this simplification, the three-connected nodes are the Cu2, Cu3, Cu4, and Cu5 atoms, the four-connected ones are the Cu1 atoms, and the six-connected ones are the $\{AsMo_{12}V_2\}$ clusters. To the best of

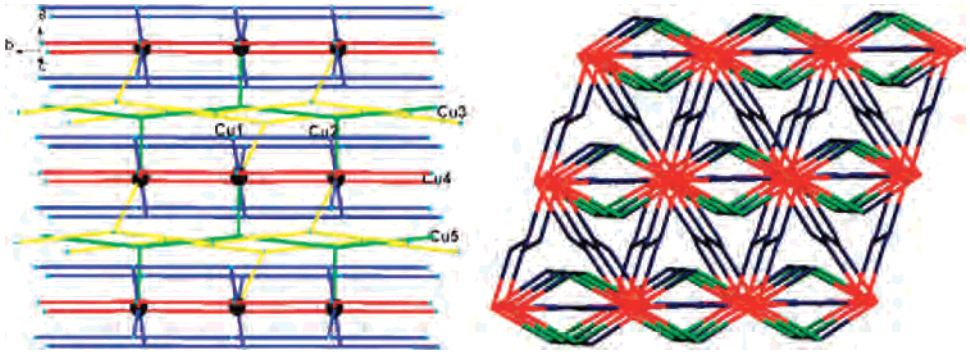

Figure 5. (left) Schematic view of the 3D framework constructed from the $\{Cu(bipy)\}_n$ chain-modified $\{AsMo_{12}V_2\}$ globes in **1**. (right) Schematic view of the $(6^2\cdot8^1)_2(8^3)_2(6^4\cdot8^2)_2(6^1\cdot8^{14})$ topology (blue, three-connected node; green, four-connected node; and red, six-connected node).

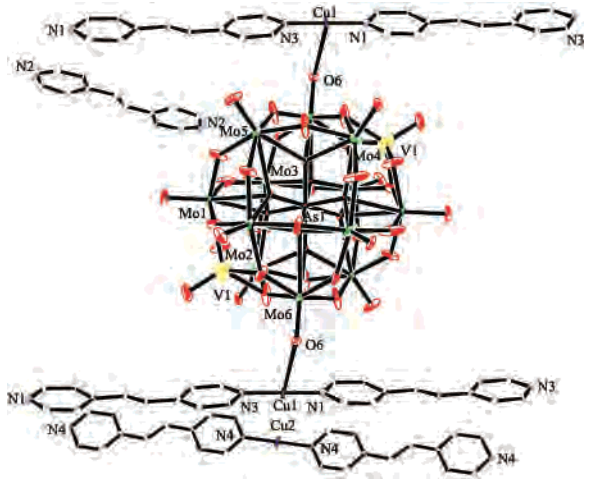

Figure 6. ORTEP drawing of the fundamental building block of compound **2** at the 30% probability level. Only some atoms are labeled, and water molecules and all hydrogen atoms are omitted for clarity.

our knowledge, this topology framework has never been observed in POM chemistry.

It should be emphasized that the successful isolation of compound **1** relies on the following factors: vanadate was used as a V resource to cap the POM cage, and the vanadium-capped POM is prone to accepting electrons, increasing the negative charge density of the POM; the different coordination environments of the two V atoms in the bicapped POM result in a more asymmetrical negative charge distribution on the POM globe; the reductant trea is moderately good at maintaining the skeleton of POMs; and the d^{10} metal ions used generally show variable coordination numbers and tunable coordination spheres. These factors combined together promote the formation of high-dimensional hybrid compounds based on multiple connected POMs with asymmetrical modification.

Structure Description of Compound 2. Compound **2** consists of three $[Cu(bpe)]^+$ moieties, one $\{AsMo_{12}O_{40}(VO)_2\}\}^{5-}$ anion (abbreviated to $\{AsMo_{12}V_2\}'$), one $[H_2bpe]^{2+}$ dication, and one water molecule. Slightly different from the $\{AsMo_{12}V_2\}$ cluster, the $\{AsMo_{12}V_2\}'$ cluster is capped by two identical {VO} units, shown in Figure 6. Additionally, the central AsO_4 tetrahedron is disordered with a half occupation of the O atoms. This kind of disorder often appears in the $[XM_{12}O_{40}]^{n-}$ Keggin clusters, which was explained by Evans and Pope[17] by stating that the disorder was a crystallographic result, namely, a single Keggin anion was superimposed by a second one by rotating 90° about a C_4 axis. There is one crystallographically unique V center and two crystallographically unique Cu centers: The V1 atom adopts a square pyramidal coordination geometry ($\tau = 0.02$) with the bond lengths of V−O ranging from 1.57(2) to 2.045 (13) Å and the O−V−O angles in the range of 77.0(5)−118.8(12)°; the Cu1 atoms adopt a three-coordinated T-type coordination geometry achieved by two N atoms from two bpe ligands and one terminal O atom (O6) from the $\{AsMo_{12}V_2\}'$ cluster, and the Cu2 atoms adopt a two-coordinated linear coordination geometry achieved by two N atoms from two bpe ligands. The bond distances and angles around Cu1 are 1.873(9)−1.880(10) Å (Cu−N), 2.587(08) Å (Cu−O6), 179.11° (N−Cu−N), and 88.00−91.18° (N−Cu−O6), and the bond distances and angles around Cu2 are 1.874(9) Å (Cu−N) and 180° (N−Cu−N).

On the other hand, each bpe molecule acting as a bridging bidentate ligand links two Cu(I) ions via its' N atoms, forming a chain. In these coordination polymeric chains, $\{Cu1(bpe)\}_n$ chains are joined together by the $\{AsMo_{12}V_2\}'$ clusters to build up a rail-like chain, in which the $\{AsMo_{12}V_2\}'$ cluster as a bridging bidentate inorganic ligand looks like the middle rail (Figure 7, left, and Supporting Information Figure S3). The adjacent "rails" are linked via weak Cu···O interactions (2.868 Å) to form a 2D structure (Figure 7, right). Furthermore, additional interactions occur between two adjacent rails through the intermediate isolated $\{Cu2(bpe)\}_n$ chain with short distances of C11···C16 (3.371 Å), and offset face-to-face $\pi\cdots\pi$ stacking (the centroid−centroid contact distance is 3.622 Å) (Figure S4, Supporting Information). Short interactions also exist among the free bpe molecule and the two adjacent $\{AsMo_{12}V_2\}'$ clusters with the shortest C···O distance of 2.893 Å (Figure S5, Supporting Information).

Comparing compound **1** with **2,** both are based on the bivanadium-capped Keggin polyoxoanions with only slight difference, while the significant difference is in the lengths of the organic ligands. The N···N distance is 9.344 Å in a bpe molecule and 7.087 Å in a bipy molecule. This will certainly lead to structural differences for compounds **1** and

(17) Evans, H. T., Jr.; Pope, M. T. *Inorg. Chem.* **1984**, *23*, 501−504.

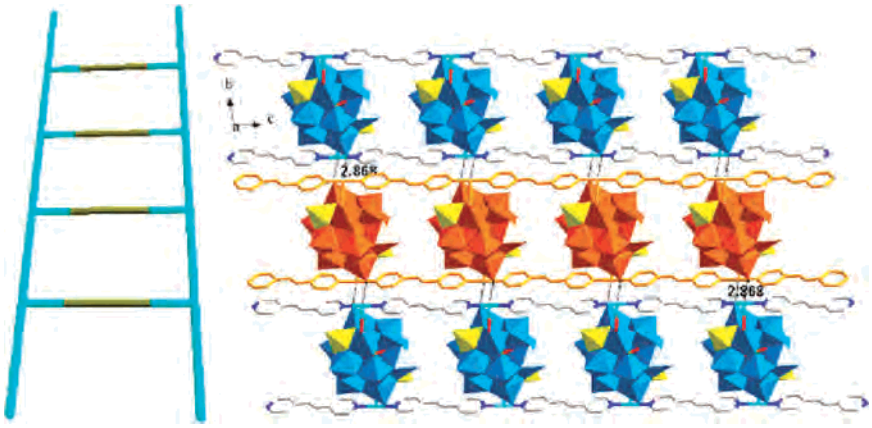

Figure 7. (left) Schematic view of rail-like double monotrack $\{Cu(bpe)\}_n$ chain-modified POMs. (right) Combined polyhedral/wire representation of the 2D layer structure via weak Cu···O interactions (2.868 Å) in **2.**

2. As mentioned above, in compound **1** the POM as a hexaconnected inorganic ligand adopts an unusually asymmetrical coordination manner. In the 3D structure, $\{AsMo_{12}V_2\}$ clusters array in an "up-and-down" mode along the $\{Cu(bipy)\}_n$ chains to avoid unfavorable interactions, making more covalent grafts of the POM with ease. Whereas in compound **2**, the longer Cu(bpe) unit is able for the $\{Cu(bpe)\}_n$ chains to accommodate $\{AsMo_{12}V_2\}'$ clusters side-by-side. This stacking mode will hinder further modification of the POMs and stop high-dimensional and high-connectivity self-assembly of the POMs with Cu−bpe complexes. Thus, a 1D structure of the double monotrack $\{Cu(bpe)\}_n$ chain-modified $\{AsMo_{12}V_2\}'$ is established for compound **2**. These results confirm again that the different lengths of spacers in the organic ligands can significantly affect the modification and assembly of the POMs with Cu−N coordination polymeric chains.

FT-IR and XPS Spectra. In the IR spectra (see Figure S6, Supporting Information), characteristic vibration peaks of the Keggin polyoxoanions are observed for ν (As−O), ν (Mo−Od), ν (Mo−Ob−Mo), and ν (Mo−Oc−Mo) at 1056, 947, 881, and 766 cm^{-1} for **1** and 1059, 944, 881, and 773 cm^{-1} for **2** (where Od = terminal O atoms, Ob = corner-sharing O atoms of two octahedra, and Oc = edge-sharing O atoms of two octahedra), respectively.[14] The characteristic absorption peaks of the bipy and bpe groups are in the 1410−1620 cm^{-1} range.

The bond valence sum (BVS) calculations[18] indicate that all Cu atoms are in the +1 oxidation state, all V atoms are in the +4 oxidation state, and 6 out of 12 Mo atoms are in the +5 oxidation state for **1** and **2**. The oxidation states of Mo, V, and Cu were further confirmed by XPS measurements, which were performed in the energy regions of Mo3d, V2p, and Cu2p, respectively. The XPS spectra (Figure S7, Supporting Information) exhibit two peaks at 933.5 and 953.2 eV for **1** and **2**, attributed to $Cu^{+}_{2p3/2}$ and $Cu^{+}_{2p5/2}$; two overlapped peaks at 232.2 and 231.2 eV for **1** and 232.4 and 231.4 eV for **2**, attributed to $Mo_{3d}{}^{6+}$ and $Mo_{3d}{}^{5+}$; and 516.2 eV for **1** and 516.7 eV for **2**, attributed to V^{4+}. These results are consistent with elemental analysis, coordination geometries, and charge balance, which confirm the structure analyses.

Note that the oxidation state of copper was changed from the reactant Cu(II) ions to the resultant Cu(I) ions, which was confirmed by BVS calculations and XPS. Such a phenomenon is often observed in the reaction of an N-containing ligand with the Cu(II) ion under hydrothermal conditions. Usually, a lower pH value and a higher reaction temperature are found to be important factors that influence the oxidation state change of the Cu ions.[19]

Cyclic Voltammetry. To study the redox properties of compounds **1** and **2**, the POM-modified CPEs (**1**−CPE and **2**−CPE) were fabricated as described in the Experimental Section. Figure 8 shows the cyclic voltammetric behaviors of **1**−CPE (left) and **2**−CPE (right) in a 1 M H_2SO_4 solution. In the voltammograms, three pairs of redox peaks (I−I′, II−II′, and III−III′) are observed for both **1** and **2**, ascribed to three consecutive redox processes of Mo. Although the $AsMo_{12}V_2$ clusters in compounds **1** and **2** are quite similar, the mean peak potentials $E_{1/2} = (E_{pc} + E_{pa})/2$ are different: −75, +177, and +398 mV for **1** and −84, +236, and +412 mV for **2**. These differences are explainable due to their different chemical environments. It is noted that there is an additional pair of redox peaks (IV−IV′) for **2**, and the mean peak potential is 542 mV. To assign the IV−IV′ redox peaks, a control experiment of bpe−CPE has been done under identical conditions. The cyclic voltammogram of bpe−CPE shows a pair of redox peaks at 514 mV (see the inset in Figure 8). In comparison with the cyclic voltammograms of **1**−CPE and bpe−CPE, we can ascribe the IV−IV′ peaks to the redox process of the bpe ligand. We have not observed redox peaks of Cu and V for both compounds, perhaps due to their weak signals embedded in the redox peaks of Mo.[13,20] With the increase of scan rate, the increasing extents of the

(18) Brown, I. D.; Altermatt, D. *Acta Crystallogr., Sect. B* **1985**, *41*, 244−247.

(19) (a) Wu, C. D.; Lu, C. Z.; Zhuang, H. H.; Huang, J. S. *Inorg. Chem.* **2002**, *41*, 5636−5637. (b) Liu, C. M.; Zhang, D. Q.; Zhu, D. B. *Cryst. Growth Des.* **2005**, *5*, 1639−1642. (c) Ren, Y. P.; Kong, X. J.; Hu, X. Y.; Sun, M.; Long, L. S.; Huang, R. B.; Zheng, L. S. *Inorg. Chem.* **2006**, *45*, 4016−4023. (d) Jin, H.; Qin, C.; Li, Y. G.; Wang, E. B. *Inorg. Chem. Commun.* **2006**, *9*, 482−485.

(20) Han, Z. G.; Zhao, Y. L.; Peng, J.; Feng, Y. Y.; Yin, J. N.; Liu, Q. *Electroanalysis* **2005**, *17*, 1097−1011.

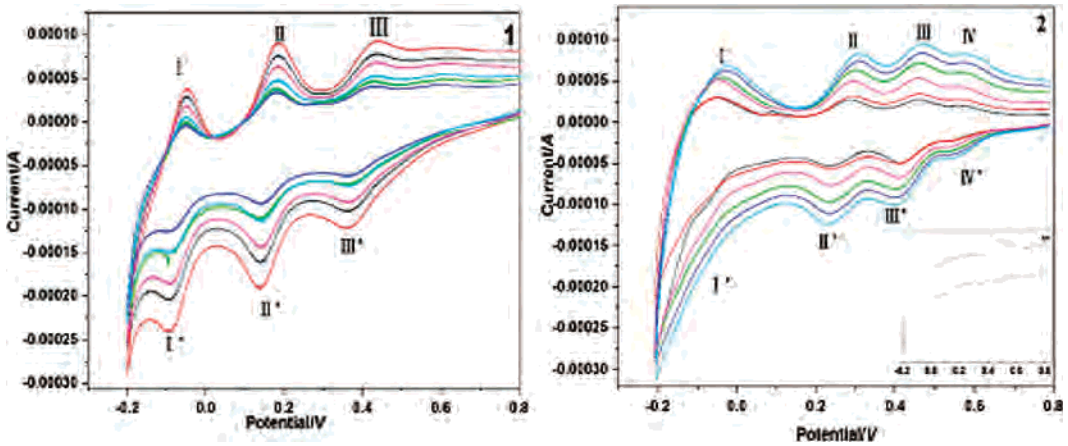

Figure 8. Cyclic voltammogram of the **1**−CPE (left) and **2**−CPE (right) in 1 M H_2SO_4 aqueous solution at different scan rates (from inner to outer: 50, 100, 150, 200, 250, and 300 mV·s^{-1}). The inset is the cyclic voltammogram of bpe−CPE in a 1 M H_2SO_4 solution at a scan rate of 50 mV·s^{-1}.

anodic and cathodic peak currents are almost the same, which indicates that the redox process is surface-controlled and the exchange rate of the electrons is faster with increasing scan rate.[21] The peak potentials change gradually: The cathodic peak potentials shift toward the negative direction and the corresponding anodic peak potentials shift toward the positive direction. The peak-to-peak separation between the corresponding cathodic and anodic peaks increases with the increasing scan rate, but the average peak potentials do not change on the whole.

Conclusion

Compounds **1** and **2** were isolated under quite similar hydrothermal conditions except for the use of different organic ligands, both of which were rigid but with different spacers. Compound **1** possesses a complicated 3D structure, in which the bivanadium-capped Keggin $\{AsMo_{12}V_2\}$ as a hexadentate inorganic ligand is modified in an unusually asymmetrical coordination mode, whereas compound **2** exhibits a rail-like 1D structure, in which $\{AsMo_{12}V_2\}'$ as a bidentate inorganic ligand is modified in a symmetrical coordination mode. In the electronic structure point of view, the bivanadium-capped Keggin polyoxoanions are prone to an asymmetrical distribution of negative charge on the POM globe, offering an opportunity to modify the POM in an asymmetrical coordination mode. In the steric hindrance point of view, $\{AsMo_{12}V_2\}$ clusters array in an up-and-down mode along the Cu−bipy chains to avoid unfavorable interactions in compound **1**. Whereas the $\{AsMo_{12}V_2\}'$ clusters adopt a side-by-side arrangement in compound **2**, which hinders the further modification of the POMs. The informative structures of the two compounds further indicate that the high-dimensional assembly of POM−TM cation coordination polymers depends on a synergic effect of polyoxoanion templates, metal ion coordination geometries, and the spacer lengths of the rigid organic ligands.

Acknowledgment. This work is financially supported by the National Natural Science Foundation of China (20671016) and the Analysis and Testing Foundation of Northeast Normal University.

Supporting Information Available: Tables of selected bond lengths (Å) and bond angles (deg) for compounds **1** and **2**; XPS, IR data, and structural figures of compounds **1** and **2**. This material is available free of charge via the Internet at http://pubs.acs.org.

IC7014308

(21) (a) Pope, M. T.; Papaconstantinou, E. *Inorg. Chem.* **1966,** *7*, 1147. (b) Han, Z. G.; Zhao, Y. L.; Peng, J.; Feng, Y. H.; Yin, J. N.; Liu, Q. *Eletroanalysis* **2002**, *17*, 1097−1102.